Exact Solution of Bipartite Fluctuations in One-Dimensional Fermions

Kazuya Fujimoto and Tomohiro Sasamoto
Department of Physics, Institute of Science Tokyo, 2-12-1 Ookayama, Meguro-ku, Tokyo 152-8551, Japan

(Received 18 April 2024; revised 3 August 2024; accepted 16 December 2024; published 12 February 2025)

Emergence of hydrodynamics in quantum many-body systems has recently garnered growing interest. The recent experiment of ultracold atoms [J. F. Wienand *et al.*, Nat. Phys. **20**, 1732 (2024)] studied emergent hydrodynamics in hard-core bosons using a bipartite fluctuation, which quantifies how the particle number fluctuates in a subsystem. In this Letter, we theoretically study the variance of a bipartite fluctuation in one-dimensional noninteracting fermionic dynamics starting from an alternating state, deriving the exact solution of the variance and its asymptotic linear growth law for the long-time dynamics. To compare the theoretical prediction with the experiment, we generalize our exact solution by incorporating the incompleteness of the initial alternating state, deriving the general linear growth law analytically. We find that it shows good agreement with the experimentally observed variance growth without any fitting parameters. Furthermore, we estimate a timescale for the local equilibration using our exact solution, finding that the timescale is independent of the initial incompleteness. To investigate the interaction effect, we implement numerical studies for the variance growth in interacting fermions, which has yet to be explored experimentally. As a result, we find that the presence of interactions breaks the linear variance growth derived in the noninteracting fermions. Our exact solutions and numerical findings here lay a foundation for growing bipartite fluctuations in quantum many-body dynamics.

DOI: 10.1103/PhysRevLett.134.067101

Introduction—Relaxation to an equilibrium state is ubiquitous in quantum many-body dynamics, bringing up fundamental and intriguing questions, e.g., how an isolated quantum system relaxes to a thermal equilibrium state [1–8]. Over decades, such quantum thermalization has been intensively studied from broad perspectives, such as the eigenstate thermalization hypothesis [9,10], integrability [11–20], many-body localization [21–32], and quantum scars [33–38]. To date, many experiments involving ultracold atoms and trapped ions have observed various phenomena related to quantum thermalization [11,12,18,20,27,31–33,39–43].

Recently, beyond the conventional quantum thermalization, hydrodynamic description based on local equilibrium has rapidly developed in quantum many-body systems. This situation is exemplified by the recent observation of electron fluids in strongly interacting systems [44–49] and the success of generalized hydrodynamics being valid for integrable quantum models [50–65]. When considering such hydrodynamic description, it is of essence to scrutinize how a system approaches a local equilibrium state. One of the most useful quantities for diagnosing local equilibrium is a bipartite fluctuation that quantifies how a physical quantity in a subsystem fluctuates. In a recent experiment of ultracold atoms for hard-core bosons [66], J. F. Wienand *et al.* utilized the bipartite fluctuation of the particle number in quench dynamics starting from the alternating state, studying the local equilibrium and the emergence of fluctuating hydrodynamics in the quantum many-body system. The experiment focused mainly on the hard-core bosons on a ladder system while also studying the ones on a one-dimensional system, which can be mapped into noninteracting fermions.

Despite the recent strong interest in emergent hydrodynamics in a quantum regime, understanding the experimentally observed bipartite fluctuation of Ref. [66] from the perspective of exact solutions is elusive even in the simplest one-dimensional hard-core bosons [67,68], although several numerical works [69–75] exist. Hence, the fundamental understanding of such bipartite fluctuations is highly desirable now, and it is of immense importance to explain the recently observed bipartite fluctuation via exact solutions.

In this Letter, we consider one-dimensional fermions starting from the alternating state, theoretically studying time evolution for the variance of the particle numbers in a subsystem as schematically shown in Fig. 1(a) and compare our theoretical prediction with the recent experimental data of Ref. [66]. First, in the noninteracting fermions, we obtain the exact and simple expression of the variance and derive the asymptotic linear growth of the variance. Second, we compare our analytical result with the experiment of Ref. [66]. For this purpose, we incorporate the incompleteness of the initial alternating state realized in the experiment into our exact solution, deriving the general linear growth law of the variance. This general law agrees well with the variance growth observed in Ref. [66] without any

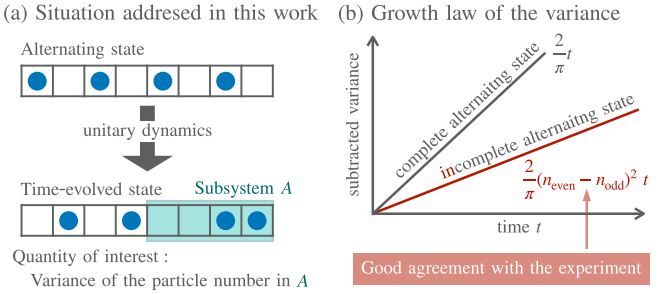

FIG. 1. Schematic illustration of the main result. (a) One-dimensional fermions addressed in this work. The blue circles represent fermions, and they occupy every other site at the initial time. This state is referred to as an alternating state. The fermions hop to neighboring sites in time. The quantity of our interest is the variance of the particle number in a subsystem A for a time-evolved state. (b) Schematic for the variance growth. The abscissa and ordinate, respectively, denote time t and a subtracted variance, which is defined by the variance from which one subtracts its initial value. The two solid lines represent our analytical results, namely, $2t/\pi$ and $2(n_{\mathrm{even}}-n_{\mathrm{odd}})^2 t/\pi$, obtained by considering the variances growing from the complete and incomplete alternating states. Here, n_{even} and n_{odd} are averaged initial particle numbers at even and odd sites, respectively, quantifying the incompleteness of the initial alternating state.

fitting parameters. The impact of the incompleteness is schematically displayed in Fig. 1(b). Furthermore, utilizing the exact solution before taking the large-size limit, we analytically estimate a timescale for the local equilibration. Finally, we numerically investigate interaction effects on the variance growth using the time-evolving block decimation (TEBD) method [76–79].

Before ending the introduction, it is worth noting that a bipartite fluctuation has been studied in terms of an integrated current and full counting statistics. In the former case, most of previous works consider dynamics starting from a domain-wall initial state, investigating a bipartite fluctuation for a conserved quantity by connecting it to an integrated current via a continuity equation [80–91]. One of the notable results is the logarithmic growth of the variance in noninteracting fermions [80]. In the latter case, a bipartite fluctuation has been employed to study static and dynamic properties of entanglement entropy [92–98] and fluctuations of physical quantities [99–109].

Setup—Let us consider fermions on a one-dimensional lattice labeled by $\Lambda := \{-L, -L+1, \ldots, L\}$ with a positive even number L. We denote the fermionic creation and annihilation operators at a site $j \in \Lambda$ by $\hat{a}_j^\dagger$ and $\hat{a}_j$. Then, the Hamiltonian is given by

$$\hat{H} := -\sum_{j=-L}^{L-1}\left(\hat{a}_{j+1}^\dagger \hat{a}_j + \hat{a}_j^\dagger \hat{a}_{j+1}\right) + U\sum_{j=-L}^{L-1}\hat{n}_{j+1}\hat{n}_j, \quad (1)$$

with the particle-number operator $\hat{n}_j := \hat{a}_j^\dagger \hat{a}_j$ and the interaction parameter U. Here, the boundary condition is basically a periodic boundary condition ($\hat{a}_L = \hat{a}_{-L}$), but we use an open boundary condition ($\hat{a}_L = 0$) in several cases. In the latter case, we will explicitly specify the boundary condition. The initial state is the alternating state defined by $|\psi_{\mathrm{alt}}\rangle := \prod_{j=-L/2}^{L/2-1}\hat{a}_{2j+1}^\dagger|0\rangle$. We denote a quantum state at time t by $|\psi(t)\rangle$ and assume that the state obeys the Schrödinger equation $id|\psi(t)\rangle/dt = \hat{H}|\psi(t)\rangle$. Here, the Dirac constant $\hbar$ is set to be unity. Note that our model with $U = 0$ is equivalent to 1D hard-core bosons. Thus, our theoretical results based on this model are relevant to experimental results for 1D hard-core bosons of Ref. [66].

In this Letter, we shall study the fluctuation of the particle number in a subsystem. The operator for the bipartite particle number is defined by $\hat{N}_M := \sum_{j=0}^{M-1}\hat{a}_j^\dagger \hat{a}_j$ with a positive integer M. Then, a generating function for the nth moment of $\hat{N}_M$ is given by $G_M(\lambda, t) := \langle e^{\lambda \hat{N}_M}\rangle_t$, where we introduce the notation $\langle \bullet \rangle_t := \mathrm{Tr}[\hat{\rho}(t)\bullet]$ with the density matrix $\hat{\rho}(t) := |\psi(t)\rangle\langle\psi(t)|$. We can compute the moments by differentiating $G_M(\lambda, t)$ with respect to λ.

Exact solution for the variance of the noninteracting fermions—We study the time evolution for the variance of $\hat{N}_M$ in the noninteracting fermions ($U = 0$) under the thermodynamic limit ($L \to \infty$). As described in Sec. I of Supplemental Material [110], the generating function $G_M(\lambda, t)$ becomes [81,96,99]

$$G_M(\lambda, t) = \det\left[\delta_{j,k} + (e^\lambda - 1)\langle \hat{a}_j^\dagger \hat{a}_k\rangle_t\right]_{j,k=0}^{M-1}. \quad (2)$$

Here, the two-point correlator $\langle \hat{a}_j^\dagger \hat{a}_k\rangle_t$ in the thermodynamic limit ($L \to \infty$) is given by [111]

$$\langle \hat{a}_j^\dagger \hat{a}_k\rangle_t = \frac{\delta_{j,k}}{2} - \frac{i^{j+k}}{2}J_{k-j}(4t). \quad (3)$$

We here derive the exact and simple expression for the variance of $\hat{N}_M$ under the limit $M \to \infty$. The first step is to express the variance via the Bessel function $J_n(x)$ of the first kind. Differentiating Eq. (2) with respect to λ, we obtain the variance $\sigma_M(t)^2 := \langle \hat{N}_M^2\rangle_t - \langle \hat{N}_M\rangle_t^2 = \partial^2 G_M(\lambda, t)/\partial\lambda^2|_{\lambda=0} - (\partial G_M(\lambda, t)/\partial\lambda|_{\lambda=0})^2$ as

$$\sigma_M(t)^2 = \frac{M}{4}\left(1 - J_0(4t)^2 - 2\sum_{k=1}^{M-1}J_k(4t)^2\right) + \frac{1}{2}\sum_{k=1}^{M-1}kJ_k(4t)^2. \quad (4)$$

The detailed derivation of Eq. (4) is given in Sec. II of Supplemental Material [110]. The next task is to take the limit $M \to \infty$ in Eq. (4). As proved in Sec. III of [110],

we have $\lim_{M\to\infty} M\left(1 - J_0(4t)^2 - 2\sum_{k=1}^{M-1} J_k(4t)^2\right)/4 = 0$ for $t > 0$ and $\lim_{M\to\infty} \sum_{k=1}^{M-1} kJ_k(4t)^2/2 = 4t^2\left(J_0(4t)^2 + J_1(4t)^2\right) - tJ_0(4t)J_1(4t)$. We utilize these formulas and Eq. (4), deriving the following exact and simple expression of the variance $\sigma(t)^2 := \lim_{M\to\infty}\sigma_M(t)^2$,

$$\sigma(t)^2 = 4t^2(J_0(4t)^2 + J_1(4t)^2) - tJ_0(4t)J_1(4t), \quad (5)$$

for $t > 0$. Note that Eq. (5) is still valid at $t = 0$ since we can show $\sigma_M(0)^2 = 0$ and $\sigma(0)^2 = 0$ from Eqs. (4) and (5), respectively. Thus, we can relax the constraint $t > 0$ for Eq. (5) to $t \geq 0$.

We apply asymptotic analysis to Eq. (5), deriving the asymptotic forms of $\sigma(t)^2$ both for the short-time ($t \ll 1$) and long-time ($t \gg 1$) dynamics. Using the asymptotic forms of the Bessel functions of the first kind [112], we obtain

$$\sigma(t)^2 \simeq \begin{cases} 2t^2 & (t \ll 1) \\ \frac{2}{\pi}t - \frac{1}{64\pi t}(2\sin(8t) + 1) & (t \gg 1). \end{cases} \quad (6)$$

The detailed derivation of Eq. (6) is given in Sec. IV of Supplemental Material [110]. The essential consequence of Eq. (6) is that the variance is proportional to time t for $t \gg 1$. This linear growth law is entirely different from the variance growth in noninteracting fermionic dynamics starting from the domain-wall state $|\psi_{\mathrm{DW}}\rangle := \prod_{j\in\mathbb{Z}_{<0}} \hat{a}_j^\dagger|0\rangle$, where the variance was shown to obey the logarithmic growth [80,83]. Note that the linear growth law was numerically confirmed in Ref. [72] and Eq. (6) gives its analytical explanation.

Finally, we numerically verify Eq. (6). Figure 2 shows the time evolution of the variance obtained by Eqs. (2) and (3) numerically. One can see the excellent agreement with Eq. (6). Note that the linear growth of the variance appears in $t \gtrsim 0.4$, though it is originally derived under $t \gg 1$. This behavior is favorable for observing the linear growth experimentally.

Comparison with the experimental result of Ref. [66]—We consider whether our theoretical prediction of the variance for the noninteracting fermions can explain the experimental result reported in Ref. [66]. For this purpose, we must note that the experiment does not realize the *complete* alternating initial state $|\psi_{\mathrm{alt}}\rangle$. To make this point clear, let us denote averaged particle numbers at the even and odd sites by n_{even} and n_{odd}. The observed imbalance parameter $I := (n_{\mathrm{odd}} - n_{\mathrm{even}})/(n_{\mathrm{even}} + n_{\mathrm{odd}})$ is about 0.91 [66], which means the existence of deviation from the *complete* alternating state since $|\psi_{\mathrm{alt}}\rangle$ has $I = 1$. This observation strongly suggests that we need to incorporate the incompleteness of the initial alternating state into the analytical results of Eqs. (5) and (6). In what follows,

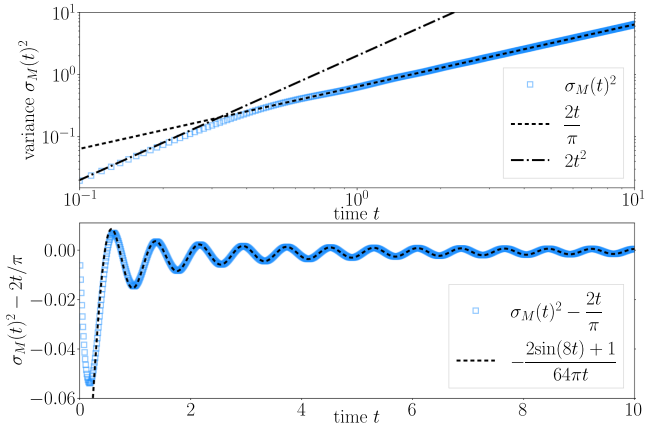

FIG. 2. Numerical verification of Eq. (6). The time evolution of the variance denoted by the blue square symbols is numerically obtained using Eqs. (2) and (3) with $M = 200$. In the upper and lower panels, we compare Eq. (6) with the numerical result.

we describe our analytical solution with the *incomplete* alternating state, comparing it with the experimental data.

Before calculating the variance, we first specify an initial state for the incomplete alternating state by considering how the alternating state is experimentally prepared. The experiment prepares the initial state by ramping up a strongly tilted double-well potential in one direction (see Sec. I. B. of Supplemental Material of Ref. [66]). Thus, we expect that the experimental initial state is well described by a product state, assuming that the initial density matrix is approximated by

$$\hat{\rho}_{\mathrm{alt}} := \frac{1}{\Xi}\exp\left(-\beta\hat{H}_{\mathrm{alt}} + \beta\mu\hat{N}_{\mathrm{tot}}\right) \quad (7)$$

with the inverse temperature β, the chemical potential μ, and the partition function $\Xi := \mathrm{Tr}\exp(-\beta\hat{H}_{\mathrm{alt}} + \beta\mu\hat{N}_{\mathrm{tot}})$. The operators $\hat{H}_{\mathrm{alt}}$ and $\hat{N}_{\mathrm{tot}}$ are defined by $\hat{H}_{\mathrm{alt}} := \sum_{j=-L/2}^{L/2-1}(\hat{a}_{2j}^\dagger\hat{a}_{2j} - \hat{a}_{2j+1}^\dagger\hat{a}_{2j+1})$ and $\hat{N}_{\mathrm{tot}} := \sum_{j=-L}^{L-1}\hat{a}_j^\dagger\hat{a}_j$. The averaged particle numbers at the even and odd sites become $n_{\mathrm{even}} = 1/[e^{\beta(1-\mu)} + 1]$ and $n_{\mathrm{odd}} = 1/[e^{\beta(-1-\mu)} + 1]$. The parameters β and μ are determined by the filling factor $\nu := (n_{\mathrm{even}} + n_{\mathrm{odd}})/2$ and the imbalance parameter I, both of which are observable in the experiment.

We analytically derive the exact and asymptotic forms of the variance for the dynamics starting from the incomplete alternating state of Eq. (7). As detailed in Sec. V of Supplemental Material [110], the two-point correlator becomes

$$\langle\hat{a}_j^\dagger\hat{a}_k\rangle_t = \frac{1}{2}(n_{\mathrm{even}} + n_{\mathrm{odd}})\delta_{j,k} + \frac{1}{2}(n_{\mathrm{even}} - n_{\mathrm{odd}})\mathrm{i}^{j+k}J_{k-j}(4t) \quad (8)$$

in the thermodynamic limit ($L \to \infty$). Here the density matrix is given by $\hat{\rho}(t) = e^{-i\hat{H}t}\hat{\rho}_{\rm alt}e^{i\hat{H}t}$ with Eq. (1) and $U = 0$. Following the derivation given in Sec. VI of Supplemental Material [110], we obtain the variance as

$$\sigma_M(t)^2 = \delta\sigma_M(t)^2 + (n_{\rm even} - n_{\rm odd})^2 \times \left[\frac{M}{4}\left(1 - J_0(4t)^2 - 2\sum_{m=1}^{M-1} J_m(4t)^2\right) + \frac{1}{2}\sum_{m=1}^{M-1} m J_m(4t)^2\right]. \quad (9)$$

with the function $\delta\sigma_M(t)^2 := M[n_{\rm even}(1-n_{\rm even}) + n_{\rm odd}(1-n_{\rm odd})]/2 + J_0(4t)[n_{\rm even}(1-n_{\rm even}) - n_{\rm odd}(1-n_{\rm odd})] \times [\sum_{m=0}^{M-1}(-1)^m]/2$. Under the setup, we can derive

$$\sigma_{\rm sub}(t)^2 := \lim_{M\to\infty}\left(\sigma_M(t)^2 - \delta\sigma_M(t)^2\right) = (n_{\rm even} - n_{\rm odd})^2\left[4t^2\left(J_0(4t)^2 + J_1(4t)^2\right) - tJ_0(4t)J_1(4t)\right]. \quad (10)$$

Here, the time-dependent term of $\delta\sigma_M(t)^2$ is much smaller than the time-independent term when M is large. Hence, we have $\delta\sigma_M(t)^2 \simeq \sigma_M(0)^2$ for $M \gg 1$. Thus $\sigma_{\rm sub}(t)^2$ can be interpreted as the variance from which one subtracts its initial value. Applying the asymptotic analysis used in Eq. (6) to Eq. (10), we derive

$$\sigma_{\rm sub}(t)^2 \simeq \begin{cases} 2(n_{\rm even} - n_{\rm odd})^2 t^2 & (t \ll 1) \\ \frac{2}{\pi}(n_{\rm even} - n_{\rm odd})^2 t & (t \gg 1). \end{cases} \quad (11)$$

This result elucidates that the incompleteness of the alternating state substantially affects the coefficient of the variance, but the exponents of time are robust.

In addition to Eq. (11), we shall compare the numerical calculations in a finite system with the experiment. Our numerical calculation is implemented for $2L = 40$, $\nu = 0.44$, and $I = 0.91$, which are taken from Ref. [66] (see Sec. II. C. of the Supplemental Material of Ref. [66]). We adopt the Hamiltonian defined by

$$\hat{H}' := -\sum_{j=-L}^{L-1}\left(\hat{a}_{j+1}^\dagger\hat{a}_j + \hat{a}_j^\dagger\hat{a}_{j+1}\right) + \sum_{j=-L}^{L-1} V_j\hat{n}_j \quad (12)$$

with the open boundary condition ($\hat{a}_L = 0$). Following the numerical simulation in Ref. [66], we here add a random potential V_j sampled from a uniform distribution with the range $[-\Delta, \Delta]$. Here, $\Delta \geq 0$ denotes the strength of the randomness. Under this setup, we investigate the variance $\sigma'_M(t)^2 := \overline{\langle\hat{N}'^2_M\rangle} - \left(\overline{\langle\hat{N}'_M\rangle}\right)^2$ with $\hat{N}'_M := \sum_{m=-M/2}^{M/2-1}\hat{a}_m^\dagger\hat{a}_m$.

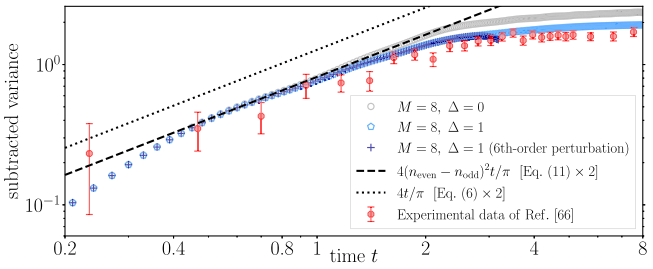

FIG. 3. Comparison of our theoretical prediction with the experimental data. The parameters are $2L = 40$, $\nu = 0.44$, $I = 0.91$, and $M = 8$, which are taken from Ref. [66]. The time evolution of the variance, denoted by circle and pentagon markers, is numerically obtained using Eq. (12) with $\Delta = 0$ and 1. For the comparison with the experiment, we plot the subtracted variance $2\sigma'_M(t)^2 - 2\sigma'_M(0)^2$ for the theoretical results and $\sigma_{\rm exp}(t)^2 - \sigma_{\rm exp}(t_0)^2$ for the experimental result because the experiment studies two-ladder lattice systems and thus the observed variance is twice as large as ours. Here, the experimental data $\sigma_{\rm exp}(t)^2$ is taken from Fig. S8 of Ref. [66], and t_0 is 0.000 603 185 789 489 2. The dotted and dashed lines correspond to our analytical expressions of Eqs. (6) and (11) for $t \gg 1$, respectively. The plus marker denotes the numerical data of the 6th order perturbative calculation.

Here, the overline $\overline{\bullet}$ denotes the ensemble average over the random potentials, and we use 10 000 samples for this.

Figure 3 compares our theoretical results with the experimental data of Ref. [66]. Our numerical result with $\Delta = 0$ can capture the variance growth in the early stage of the dynamics, but the deviation from the experimental data grows in time. On the other hand, when we turn on the random potential with $\Delta = 1$, the numerical result well reproduces the experimental data. The saturation of the variance for $t \gtrsim 2$ is caused by the finite size effect and the disorder potential. These behaviors were reported in the numerical simulations of Ref. [66]. We also implement a numerical perturbative calculation with Δ, finding that the 6th order perturbative result well describes the time evolution before the saturation (see Sec. VII of Supplemental Material [110] for the detailed numerical method). Comparing these results, one can see that the disorder effect is irrelevant in $t \lesssim 1$.

The dotted and dashed lines in Fig. 3 show the analytical results for the linear growth of Eqs. (6) and (11). We find that the latter including the incompleteness of the initial alternating state exhibits good agreement with the experimental linear growth, while the former, not including the incompleteness, systematically deviates from the experimental data. We here emphasize that our analytical result (11) agrees well with the experimental data without any fitting parameters under the assumption of (7). Note that one can see that the disorder effect emerges before the finite M effect by comparing the numerical data for $\Delta = 0$ and 1 with Eq. (11), though the localization length is larger than $M = 8$ [66].

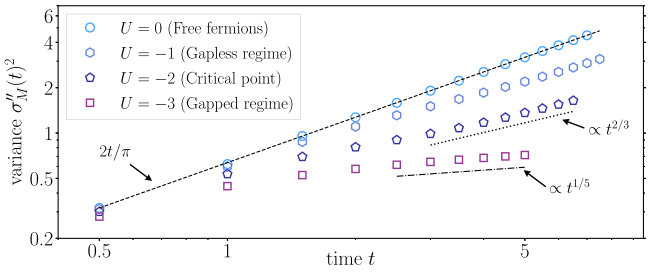

FIG. 4. Numerical results for the variance $\sigma''_M(t)^2$ with $M = 40$. The number of the lattice is $2L = 120$. We numerically solve the Schrödinger equation using the TEBD method [76–79], calculating the variances for $U = 0, -1, -2$, and -3. The dashed line denotes the leading term of Eq. (6) for $t \gg 1$, and the dotted and dot-dashed lines are curves for $t^{2/3}$ and $t^{1/5}$, respectively. We insert these curves with the exponents $2/3$ and $1/5$ for reference.

We comment on the fact that our incomplete initial density matrix of Eq. (7) cannot describe superpositions of quantum states between different sites. The experiment of Ref. [66] is expected to suppress such entangled states since deep optical lattices are used for the initial state preparation, but we numerically study the effects of the superpositions on the variance growth by extending Eq. (7) to a more general state. As illustrated in Sec. VIII of Supplemental Material [110], we numerically confirm that the results of Eq. (7) show better agreement with the experiment than ones of the general state. This finding strengthens the justification for using Eq. (7).

Finally, we discuss a timescale for local equilibration on the basis of our exact solution of Eq. (9) for a finite $M \gg 1$, where the linear growth of the subtracted variance, namely, $2(n_{\mathrm{even}} - n_{\mathrm{odd}})^2 t/\pi$, becomes dominant [see Eq. (11)]. When taking the long-time limit of Eq. (9), we obtain the stationary value of the subtracted variance $\lim_{t\to\infty}[\sigma_M(t)^2 - \delta\sigma_M(t)^2] = (n_{\mathrm{even}} - n_{\mathrm{odd}})^2 M/4$. Then, we can estimate the local equilibration time T_* by equating the expressions for these two subtracted variances, finding $T_* \sim \pi M/8$. Interestingly, our exact solution leads to the fact that T_* is independent of the initial value of $n_{\mathrm{even}} - n_{\mathrm{odd}}$.

Numerical study for the variance growth of the interacting fermions—We numerically study the interaction effect on the time evolution of the variance. Our numerical method is the TEBD method [76–79] with Eq. (1) and the open boundary condition ($\hat{a}_L = 0$). We set L to be 60, and compute the variance for $U = 0, -1, -2$, and -3. In the language of the XXZ chain, $U = -2$ corresponds to the critical point at which the model is identical to the XXX chain [113]. To weaken the boundary effect, we use the variance $\sigma''_M(t)^2 := \langle(\hat{N}'_M)^2\rangle_t - \langle\hat{N}'_M\rangle_t^2$ with $M = 40$. The dependence on the bond dimensions and the time resolutions of our numerical calculations is described in Sec. X of Supplemental Material [110].

Figure 4 displays the time evolution of the variance $\sigma''_M(t)^2$. In the noninteracting fermions ($U = 0$), our numerical result for the finite system well reproduces the leading term of Eq. (6) for the infinite system. This demonstrates that the boundary effect is negligible. In the interacting cases ($U \neq 0$), the time evolution exhibits different growth behaviors, and we cannot find the clear ballistic property, particularly for the $U = -2$ and -3 cases.

Note that Cecile *et al.* recently reported similar numerical results for the variance in the XXZ chain [73]. For example, they confirmed the signature of the anomalous power law growth ($\sigma''_M(t)^2 \propto t^{2/3}$) in the dynamics starting from the Néel state identical to the alternating state. The similar signature was also discussed in Ref. [69]. We here display Fig. 4 to show that our analytical result for the noninteracting fermions does not work in the interacting cases.

Finally, we study the effect of the random potential on the variance growth. We numerically find that the disorder effect emerges in the early stage of the dynamics and the power-law-like growth in Fig. 4 becomes unclear, as described in Sec. IX of Supplemental Material [110]. This numerical finding suggests that one needs to decrease the strength of the random potential to observe the power-law-like growth in the interacting fermions, namely, the XXZ model.

Future prospects—Our theoretical results, based upon the exact solutions of the noninteracting fermions and the numerical findings of the interacting fermions will stimulate further research on emergent hydrodynamics and local equilibration of quantum many-body systems. As a prospect, it is fascinating to analytically comprehend the interaction effect via generalized hydrodynamics [50–65] and ballistic macroscopic fluctuation theory [114,115]. In another direction, it is worth studying the variance growth in open quantum systems. Depending on the kinds of interactions with environments, an open quantum system approaches a nonequilibrium stationary state being different from the equilibrium state addressed in this work. Thus, uncovering features of the variance growth in such a case is fundamentally intriguing.

Note added—Recently, Gamayun reported that the bipartite fluctuations growing from the alternating state is related to that from the domain-wall state [116].

Acknowledgments—K. F. is grateful to Ryusuke Hamazaki and Yuki Kawaguchi for fruitful discussions and comments on the manuscript, Masaya Kunimi for helpful discussions on TEBD with a conserved quantity, and Hiroki Moriya for helpful discussions. K. F. and T. S. are grateful to Monika Aidelsburger, Immanuel Bloch, Alexander Impertro, Simon Karch, Christian Schweizer, and Julian F. Wienand for sharing the experimental data. The work of K. F. has been supported by JSPS KAKENHI Grant No. JP23K13029. The work of T. S. has been supported by JSPS KAKENHI Grants No. JP21H04432, No. JP22H01143, and No. JP23K22414.

[1] A. Polkovnikov, K. Sengupta, A. Silva, and M. Vengalattore, Colloquium: Nonequilibrium dynamics of closed interacting quantum systems, Rev. Mod. Phys. **83**, 863 (2011).

[2] J. Eisert, M. Friesdorf, and C. Gogolin, Quantum many-body systems out of equilibrium, Nat. Phys. **11**, 124 (2015).

[3] R. Nandkishore and D. A. Huse, Many-body localization and thermalization in quantum statistical mechanics, Annu. Rev. Condens. Matter Phys. **6**, 15 (2015).

[4] E. J. Torres-Herrera, D. Kollmar, and L. F. Santos, Relaxation and thermalization of isolated many-body quantum systems, Phys. Scri. **2015**, 014018 (2015).

[5] A. P. Luca D'Alessio, Yariv Kafri, and M. Rigol, From quantum chaos and eigenstate thermalization to statistical mechanics and thermodynamics, Adv. Phys. **65**, 239 (2016).

[6] T. Mori, T. N. Ikeda, E. Kaminishi, and M. Ueda, Thermalization and prethermalization in isolated quantum systems: A theoretical overview, J. Phys. B **51**, 112001 (2018).

[7] D. A. Abanin, E. Altman, I. Bloch, and M. Serbyn, Colloquium: Many-body localization, thermalization, and entanglement, Rev. Mod. Phys. **91**, 021001 (2019).

[8] Z. Gong and R. Hamazaki, Bounds in nonequilibrium quantum dynamics, Int. J. Mod. Phys. B **36**, 2230007 (2022).

[9] J. M. Deutsch, Quantum statistical mechanics in a closed system, Phys. Rev. A **43**, 2046 (1991).

[10] M. Srednicki, Chaos and quantum thermalization, Phys. Rev. E **50**, 888 (1994).

[11] T. Kinoshita, T. Wenger, and D. S. Weiss, A quantum Newton's cradle, Nature (London) **440**, 900 (2006).

[12] M. Gring, M. Kuhnert, T. Langen, T. Kitagawa, B. Rauer, M. Schreitl, I. Mazets, D. A. Smith, E. Demler, and J. Schmiedmayer, Relaxation and prethermalization in an isolated quantum system, Science **337**, 1318 (2012).

[13] M. A. Cazalilla, Effect of suddenly turning on interactions in the Luttinger model, Phys. Rev. Lett. **97**, 156403 (2006).

[14] M. Rigol, A. Muramatsu, and M. Olshanii, Hard-core bosons on optical superlattices: Dynamics and relaxation in the superfluid and insulating regimes, Phys. Rev. A **74**, 053616 (2006).

[15] M. Rigol, V. Dunjko, V. Yurovsky, and M. Olshanii, Relaxation in a completely integrable many-body quantum system: An *ab initio* study of the dynamics of the highly excited states of 1D lattice hard-core bosons, Phys. Rev. Lett. **98**, 050405 (2007).

[16] P. Calabrese, F. H. L. Essler, and M. Fagotti, Quantum quench in the transverse-field Ising chain, Phys. Rev. Lett. **106**, 227203 (2011).

[17] M. Fagotti and F. H. L. Essler, Reduced density matrix after a quantum quench, Phys. Rev. B **87**, 245107 (2013).

[18] T. Langen, S. Erne, R. Geiger, B. Rauer, T. Schweigler, M. Kuhnert, W. Rohringer, I. E. Mazets, T. Gasenzer, and J. Schmiedmayer, Experimental observation of a generalized Gibbs ensemble, Science **348**, 207 (2015).

[19] E. Ilievski, J. De Nardis, B. Wouters, J.-S. Caux, F. H. L. Essler, and T. Prosen, Complete generalized Gibbs ensembles in an interacting theory, Phys. Rev. Lett. **115**, 157201 (2015).

[20] Y. Tang, W. Kao, K.-Y. Li, S. Seo, K. Mallayya, M. Rigol, S. Gopalakrishnan, and B. L. Lev, Thermalization near integrability in a dipolar quantum Newton's cradle, Phys. Rev. X **8**, 021030 (2018).

[21] D. Basko, I. Aleiner, and B. Altshuler, Metal–insulator transition in a weakly interacting many-electron system with localized single-particle states, Ann. Phys. (Amsterdam) **321**, 1126 (2006).

[22] M. Žnidarič, T. Prosen, and P. Prelovšek, Many-body localization in the Heisenberg XXZ magnet in a random field, Phys. Rev. B **77**, 064426 (2008).

[23] A. Pal and D. A. Huse, Many-body localization phase transition, Phys. Rev. B **82**, 174411 (2010).

[24] J. H. Bardarson, F. Pollmann, and J. E. Moore, Unbounded growth of entanglement in models of many-body localization, Phys. Rev. Lett. **109**, 017202 (2012).

[25] M. Serbyn, Z. Papić, and D. A. Abanin, Local conservation laws and the structure of the many-body localized states, Phys. Rev. Lett. **111**, 127201 (2013).

[26] D. A. Huse, R. Nandkishore, and V. Oganesyan, Phenomenology of fully many-body-localized systems, Phys. Rev. B **90**, 174202 (2014).

[27] M. Schreiber, S. S. Hodgman, P. Bordia, H. P. Lüschen, M. H. Fischer, R. Vosk, E. Altman, U. Schneider, and I. Bloch, Observation of many-body localization of interacting fermions in a quasirandom optical lattice, Science **349**, 842 (2015).

[28] A. C. Potter, R. Vasseur, and S. A. Parameswaran, Universal properties of many-body delocalization transitions, Phys. Rev. X **5**, 031033 (2015).

[29] R. Vasseur and J. E. Moore, Nonequilibrium quantum dynamics and transport: From integrability to many-body localization, J. Stat. Mech. (2016) 064010.

[30] J. yoon Choi, S. Hild, J. Zeiher, P. Schauß, A. Rubio-Abadal, T. Yefsah, V. Khemani, D. A. Huse, I. Bloch, and C. Gross, Exploring the many-body localization transition in two dimensions, Science **352**, 1547 (2016).

[31] H. P. Lüschen, P. Bordia, S. Scherg, F. Alet, E. Altman, U. Schneider, and I. Bloch, Observation of slow dynamics near the many-body localization transition in one-dimensional quasiperiodic systems, Phys. Rev. Lett. **119**, 260401 (2017).

[32] T. Kohlert, S. Scherg, X. Li, H. P. Lüschen, S. Das Sarma, I. Bloch, and M. Aidelsburger, Observation of many-body localization in a one-dimensional system with a single-particle mobility edge, Phys. Rev. Lett. **122**, 170403 (2019).

[33] H. Bernien, S. Schwartz, A. Keesling, H. Levine, A. Omran, H. Pichler, S. Choi, A. S. Zibrov, M. Endres, M. Greiner, V. Vuletić, and M. D. Lukin, Probing many-body dynamics on a 51-atom quantum simulator, Nature (London) **551**, 579 (2017).

[34] N. Shiraishi and T. Mori, Systematic construction of counterexamples to the eigenstate thermalization hypothesis, Phys. Rev. Lett. **119**, 030601 (2017).

[35] C. J. Turner, A. A. Michailidis, D. A. Abanin, M. Serbyn, and Z. Papić, Weak ergodicity breaking from quantum many-body scars, Nat. Phys. **14**, 745 (2018).

[36] C. J. Turner, A. A. Michailidis, D. A. Abanin, M. Serbyn, and Z. Papić, Quantum scarred eigenstates in a Rydberg

atom chain: Entanglement, breakdown of thermalization, and stability to perturbations, Phys. Rev. B **98**, 155134 (2018).
[37] C.-J. Lin and O. I. Motrunich, Exact quantum many-body scar states in the Rydberg-blockaded atom chain, Phys. Rev. Lett. **122**, 173401 (2019).
[38] N. Shibata, N. Yoshioka, and H. Katsura, Onsager's scars in disordered spin chains, Phys. Rev. Lett. **124**, 180604 (2020).
[39] S. Trotzky, Y.-A. Chen, A. Flesch, I. P. McCulloch, U. Schollwöck, J. Eisert, and I. Bloch, Probing the relaxation towards equilibrium in an isolated strongly correlated one-dimensional Bose gas, Nat. Phys. **8**, 325 (2012).
[40] T. Langen, R. Geiger, M. Kuhnert, B. Rauer, and J. Schmiedmayer, Local emergence of thermal correlations in an isolated quantum many-body system, Nat. Phys. **9**, 640 (2013).
[41] G. Clos, D. Porras, U. Warring, and T. Schaetz, Time-resolved observation of thermalization in an isolated quantum system, Phys. Rev. Lett. **117**, 170401 (2016).
[42] A. M. Kaufman, M. E. Tai, A. Lukin, M. Rispoli, R. Schittko, P. M. Preiss, and M. Greiner, Quantum thermalization through entanglement in an isolated many-body system, Science **353**, 794 (2016).
[43] C. Neill, P. Roushan, M. Fang, Y. Chen, M. Kolodrubetz, Z. Chen, A. Megrant, R. Barends, B. Campbell, B. Chiaro, A. Dunsworth, E. Jeffrey, J. Kelly, J. Mutus, P. J. J. O'Malley, C. Quintana, D. Sank, A. Vainsencher, J. Wenner, T. C. White, A. Polkovnikov, and J. M. Martinis, Ergodic dynamics and thermalization in an isolated quantum system, Nat. Phys. **12**, 1037 (2016).
[44] P. J. W. Moll, P. Kushwaha, N. Nandi, B. Schmidt, and A. P. Mackenzie, Evidence for hydrodynamic electron flow in $PdCo)_2$, Science **351**, 1061 (2016).
[45] D. A. Bandurin, I. Torre, R. K. Kumar, M. B. Shalom, A. Tomadin, A. Principi, G. H. Auton, E. Khestanova, K. S. Novoselov, I. V. Grigorieva, L. A. Ponomarenko, A. K. Geim, and M. Polini, Negative local resistance caused by viscous electron backflow in graphene, Science **351**, 1055 (2016).
[46] J. Gooth, F. Menges, N. Kumar, V. Süß, C. Shekhar, Y. Sun, U. Drechsler, R. Zierold, C. Felser, and B. Gotsmann, Thermal and electrical signatures of a hydrodynamic electron fluid in tungsten diphosphide, Nat. Commun. **9**, 4093 (2018).
[47] R. Krishna Kumar, D. A. Bandurin, F. M. D. Pellegrino, Y. Cao, A. Principi, H. Guo, G. H. Auton, M. Ben Shalom, L. A. Ponomarenko, G. Falkovich, K. Watanabe, T. Taniguchi, I. V. Grigorieva, L. S. Levitov, M. Polini, and A. K. Geim, Superballistic flow of viscous electron fluid through graphene constrictions, Nat. Phys. **13**, 1182 (2017).
[48] J. A. Sulpizio, L. Ella, A. Rozen, J. Birkbeck, D. J. Perello, D. Dutta, M. Ben-Shalom, T. Taniguchi, K. Watanabe, T. Holder, R. Queiroz, A. Principi, A. Stern, T. Scaffidi, A. K. Geim, and S. Ilani, Visualizing poiseuille flow of hydrodynamic electrons, Nature (London) **576**, 75 (2019).
[49] A. Aharon-Steinberg, T. Völkl, A. Kaplan, A. K. Pariari, I. Roy, T. Holder, Y. Wolf, A. Y. Meltzer, Y. Myasoedov, M. E. Huber, B. Yan, G. Falkovich, L. S. Levitov, M. Hücker, and E. Zeldov, Direct observation of vortices in an electron fluid, Nature (London) **607**, 74 (2022).
[50] O. A. Castro-Alvaredo, B. Doyon, and T. Yoshimura, Emergent hydrodynamics in integrable quantum systems out of equilibrium, Phys. Rev. X **6**, 041065 (2016).
[51] B. Bertini, M. Collura, J. De Nardis, and M. Fagotti, Transport in out-of-equilibrium XXZ chains: Exact profiles of charges and currents, Phys. Rev. Lett. **117**, 207201 (2016).
[52] V. B. Bulchandani, R. Vasseur, C. Karrasch, and J. E. Moore, Solvable hydrodynamics of quantum integrable systems, Phys. Rev. Lett. **119**, 220604 (2017).
[53] V. B. Bulchandani, R. Vasseur, C. Karrasch, and J. E. Moore, Bethe-Boltzmann hydrodynamics and spin transport in the XXZ chain, Phys. Rev. B **97**, 045407 (2018).
[54] B. Doyon and T. Yoshimura, A note on generalized hydrodynamics: Inhomogeneous fields and other concepts, SciPost Phys. **2**, 014 (2017).
[55] B. Doyon, J. Dubail, R. Konik, and T. Yoshimura, Large-scale description of interacting one-dimensional Bose gases: Generalized hydrodynamics supersedes conventional hydrodynamics, Phys. Rev. Lett. **119**, 195301 (2017).
[56] B. Doyon, T. Yoshimura, and J.-S. Caux, Soliton gases and generalized hydrodynamics, Phys. Rev. Lett. **120**, 045301 (2018).
[57] M. Collura, A. De Luca, and J. Viti, Analytic solution of the domain-wall nonequilibrium stationary state, Phys. Rev. B **97**, 081111(R) (2018).
[58] J. De Nardis, D. Bernard, and B. Doyon, Hydrodynamic diffusion in integrable systems, Phys. Rev. Lett. **121**, 160603 (2018).
[59] M. Schemmer, I. Bouchoule, B. Doyon, and J. Dubail, Generalized hydrodynamics on an atom chip, Phys. Rev. Lett. **122**, 090601 (2019).
[60] S. Gopalakrishnan and R. Vasseur, Kinetic theory of spin diffusion and superdiffusion in XXZ spin chains, Phys. Rev. Lett. **122**, 127202 (2019).
[61] B. Doyon, Lecture notes on generalised hydrodynamics, SciPost Phys. Lect. Notes 18 (2020).
[62] V. Alba, B. Bertini, M. Fagotti, L. Piroli, and P. Ruggiero, Generalized-hydrodynamic approach to inhomogeneous quenches: Correlations, entanglement and quantum effects, J. Stat. Mech. (2021) 114004.
[63] N. Malvania, Y. Zhang, Y. Le, J. Dubail, M. Rigol, and D. S. Weiss, Generalized hydrodynamics in strongly interacting 1D Bose gases, Science **373**, 1129 (2021).
[64] I. Bouchoule and J. Dubail, Generalized hydrodynamics in the one-dimensional Bose gas: Theory and experiments, J. Stat. Mech. (2022) 014003.
[65] F. H. Essler, A short introduction to generalized hydrodynamics, Physica (Amsterdam) **631**, 127572 (2023).
[66] J. F. Wienand, S. Karch, A. Impertro, C. Schweizer, E. McCulloch, R. Vasseur, S. Gopalakrishnan, M. Aidelsburger, and I. Bloch, Emergence of fluctuating hydrodynamics in chaotic quantum systems, Nat. Phys. **20**, 1732 (2024).
[67] S. Groha, F. H. L. Essler, and P. Calabrese, Full counting statistics in the transverse field Ising chain, SciPost Phys. **4**, 043 (2018).

[68] In Ref. [67], a probability function for the bipartite fluctuation of a transverse Ising chain was analytically studied, but this model is different from the experimental situation.
[69] K. Fujimoto, R. Hamazaki, and Y. Kawaguchi, Family-Vicsek scaling of roughness growth in a strongly interacting Bose gas, Phys. Rev. Lett. **124**, 210604 (2020).
[70] T. Jin, A. Krajenbrink, and D. Bernard, From stochastic spin chains to quantum Kardar-Parisi-Zhang dynamics, Phys. Rev. Lett. **125**, 040603 (2020).
[71] K. Fujimoto, R. Hamazaki, and Y. Kawaguchi, Dynamical scaling of surface roughness and entanglement entropy in disordered fermion models, Phys. Rev. Lett. **127**, 090601 (2021).
[72] K. Fujimoto, R. Hamazaki, and Y. Kawaguchi, Impact of dissipation on universal fluctuation dynamics in open quantum systems, Phys. Rev. Lett. **129**, 110403 (2022).
[73] G. Cecile, J. De Nardis, and E. Ilievski, Squeezed ensembles and anomalous dynamic roughening in interacting integrable chains, Phys. Rev. Lett. **132**, 130401 (2024).
[74] S. Aditya and N. Roy, Family-Vicsek dynamical scaling and Kardar-Parisi-Zhang-like superdiffusive growth of surface roughness in a driven one-dimensional quasiperiodic model, Phys. Rev. B **109**, 035164 (2024).
[75] D. S. Bhakuni and Y. B. Lev, Dynamic scaling relation in quantum many-body systems, Phys. Rev. B **110**, 014203 (2024).
[76] G. Vidal, Efficient classical simulation of slightly entangled quantum computations, Phys. Rev. Lett. **91**, 147902 (2003).
[77] G. Vidal, Efficient simulation of one-dimensional quantum many-body systems, Phys. Rev. Lett. **93**, 040502 (2004).
[78] U. Schollwöck, The density-matrix renormalization group in the age of matrix product states, Ann. Phys. (Amsterdam) **326**, 96 (2011).
[79] S. Paeckel, T. Köhler, A. Swoboda, S. R. Manmana, U. Schollwöck, and C. Hubig, Time-evolution methods for matrix-product states, Ann. Phys. (Amsterdam) **411**, 167998 (2019).
[80] T. Antal, P. L. Krapivsky, and A. Rákos, Logarithmic current fluctuations in nonequilibrium quantum spin chains, Phys. Rev. E **78**, 061115 (2008).
[81] V. Eisler and Z. Rácz, Full counting statistics in a propagating quantum front and random matrix spectra, Phys. Rev. Lett. **110**, 060602 (2013).
[82] M. Ljubotina, M. Žnidarič, and T. Prosen, Spin diffusion from an inhomogeneous quench in an integrable system, Nat. Commun. **8**, 16117 (2017).
[83] H. Moriya, R. Nagao, and T. Sasamoto, Exact large deviation function of spin current for the one dimensional XX spin chain with domain wall initial condition, J. Stat. Mech. (2019) 063105.
[84] O. Gamayun, O. Lychkovskiy, and J.-S. Caux, Fredholm determinants, full counting statistics and Loschmidt echo for domain wall profiles in one-dimensional free fermionic chains, SciPost Phys. **8**, 036 (2020).
[85] T. Jin, T. Gautié, A. Krajenbrink, P. Ruggiero, and T. Yoshimura, Interplay between transport and quantum coherences in free fermionic systems, J. Phys. A **54**, 404001 (2021).
[86] S. Gopalakrishnan and R. Vasseur, Anomalous transport from hot quasiparticles in interacting spin chains, Rep. Prog. Phys. **86**, 036502 (2023).
[87] D. Wei, A. Rubio-Abadal, B. Ye, F. Machado, J. Kemp, K. Srakaew, S. Hollerith, J. Rui, S. Gopalakrishnan, N. Y. Yao, I. Bloch, and J. Zeiher, Quantum gas microscopy of Kardar-Parisi-Zhang superdiffusion, Science **376**, 716 (2022).
[88] Ž. Krajnik, E. Ilievski, and T. Prosen, Absence of normal fluctuations in an integrable magnet, Phys. Rev. Lett. **128**, 090604 (2022).
[89] Ž. Krajnik, J. Schmidt, V. Pasquier, E. Ilievski, and T. Prosen, Exact anomalous current fluctuations in a deterministic interacting model, Phys. Rev. Lett. **128**, 160601 (2022).
[90] Ž. Krajnik, J. Schmidt, E. Ilievski, and T. Prosen, Dynamical criticality of magnetization transfer in integrable spin chains, Phys. Rev. Lett. **132**, 017101 (2024).
[91] Ž. Krajnik, J. Schmidt, V. Pasquier, T. Prosen, and E. Ilievski, Universal anomalous fluctuations in charged single-file systems, Phys. Rev. Res. **6**, 013260 (2024).
[92] I. Klich and L. Levitov, Quantum noise as an entanglement meter, Phys. Rev. Lett. **102**, 100502 (2009).
[93] H. F. Song, S. Rachel, and K. Le Hur, General relation between entanglement and fluctuations in one dimension, Phys. Rev. B **82**, 012405 (2010).
[94] H. F. Song, S. Rachel, C. Flindt, I. Klich, N. Laflorencie, and K. Le Hur, Bipartite fluctuations as a probe of many-body entanglement, Phys. Rev. B **85**, 035409 (2012).
[95] S. Rachel, N. Laflorencie, H. F. Song, and K. Le Hur, Detecting quantum critical points using bipartite fluctuations, Phys. Rev. Lett. **108**, 116401 (2012).
[96] G. Parez, R. Bonsignori, and P. Calabrese, Quasiparticle dynamics of symmetry-resolved entanglement after a quench: Examples of conformal field theories and free fermions, Phys. Rev. B **103**, L041104 (2021).
[97] H. Oshima and Y. Fuji, Charge fluctuation and charge-resolved entanglement in a monitored quantum circuit with U(1) symmetry, Phys. Rev. B **107**, 014308 (2023).
[98] B. Bertini, P. Calabrese, M. Collura, K. Klobas, and C. Rylands, Nonequilibrium full counting statistics and symmetry-resolved entanglement from space-time duality, Phys. Rev. Lett. **131**, 140401 (2023).
[99] K. Schönhammer, Full counting statistics for noninteracting fermions: Exact results and the Levitov-Lesovik formula, Phys. Rev. B **75**, 205329 (2007).
[100] M. Collura, F. H. L. Essler, and S. Groha, Full counting statistics in the spin-1/2 Heisenberg XXZ chain, J. Phys. A **50**, 414002 (2017).
[101] J.-M. Stéphan and F. Pollmann, Full counting statistics in the Haldane-Shastry chain, Phys. Rev. B **95**, 035119 (2017).
[102] K. Najafi and M. A. Rajabpour, Full counting statistics of the subsystem energy for free fermions and quantum spin chains, Phys. Rev. B **96**, 235109 (2017).

[103] M. Arzamasovs and D. M. Gangardt, Full counting statistics and large deviations in a thermal 1D Bose gas, Phys. Rev. Lett. **122**, 120401 (2019).
[104] P. Calabrese, M. Collura, G. D. Giulio, and S. Murciano, Full counting statistics in the gapped XXZ spin chain, Europhys. Lett. **129**, 60007 (2020).
[105] F. Ares, M. A. Rajabpour, and J. Viti, Exact full counting statistics for the staggered magnetization and the domain walls in the XY spin chain, Phys. Rev. E **103**, 042107 (2021).
[106] N. R. Smith, P. L. Doussal, S. N. Majumdar, and G. Schehr, Full counting statistics for interacting trapped fermions, SciPost Phys. **11**, 110 (2021).
[107] E. McCulloch, J. De Nardis, S. Gopalakrishnan, and R. Vasseur, Full counting statistics of charge in chaotic many-body quantum systems, Phys. Rev. Lett. **131**, 210402 (2023).
[108] G. Hercé, J.-P. Bureik, A. Ténart, A. Aspect, A. Dareau, and D. Clément, Full counting statistics of interacting lattice gases after an expansion: The role of condensate depletion in many-body coherence, Phys. Rev. Res. **5**, L012037 (2023).
[109] B. Bertini, K. Klobas, M. Collura, P. Calabrese, and C. Rylands, Dynamics of charge fluctuations from asymmetric initial states, Phys. Rev. B **109**, 184312 (2024).
[110] See Supplemental Material at http://link.aps.org/supplemental/10.1103/PhysRevLett.134.067101 for (I) Derivation of Eq. (2), (II) Derivation of Eq. (4), (III) Derivation of the two limiting formulas, (IV) Derivation of Eq. (6), (V) Derivation of Eq. (8), (VI) Derivation of Eq. (9), (VII) Numerical perturbative calculation for the disorder potential, (VIII) Effect of the superposition of the initial state in the noninteracting fermions, (IX) Effect of the random potential on the interacting fermions, and (X) Dependence on the bond dimension and the time resolution in the numerical calculations.
[111] A. Flesch, M. Cramer, I. P. McCulloch, U. Schollwöck, and J. Eisert, Probing local relaxation of cold atoms in optical superlattices, Phys. Rev. A **78**, 033608 (2008).
[112] 8—Special functions, in *Table of Integrals, Series, and Products (Eighth Edition)*, eighth edition ed., edited by D. Zwillinger, V. Moll, I. Gradshteyn, and I. Ryzhik (Academic Press, Boston, 2015), pp. 867–1013.
[113] F. Franchini, *An Introduction to Integrable Techniques for One-Dimensional Quantum Systems* (Springer, New York, 2017), Vol. 940.
[114] B. Doyon, G. Perfetto, T. Sasamoto, and T. Yoshimura, Emergence of hydrodynamic spatial long-range correlations in nonequilibrium many-body systems, Phys. Rev. Lett. **131**, 027101 (2023).
[115] B. Doyon, G. Perfetto, T. Sasamoto, and T. Yoshimura, Ballistic macroscopic fluctuation theory, SciPost Phys. **15**, 136 (2023).
[116] O. Gamayun, A note on "Exact solution of bipartite fluctuations in one-dimensional fermions," arXiv:2404.06881.